

Efficient purification protocols using *i*SWAP gates in solid-state qubitsTetsufumi Tanamoto,¹ Koji Maruyama,² Yu-xi Liu,^{2,3} Xuedong Hu,⁴ and Franco Nori^{2,3,5}¹*Corporate R & D Center, Toshiba Corporation, Saiwai-ku, Kawasaki 212-8582, Japan*²*Advanced Science Institute, The Institute of Physical and Chemical Research (RIKEN), Wako-shi, Saitama 351-0198, Japan*³*CREST, Japan Science and Technology Agency (JST), Kawaguchi, Saitama 332-0012, Japan*⁴*Department of Physics, University at Buffalo, SUNY, Buffalo, New York 14260-1500, USA*⁵*Physics Department, Center for Theoretical Physics, Center for the Study of Complex Systems, The University of Michigan, Ann Arbor, Michigan 48109-1040, USA*

(Received 19 August 2008; published 5 December 2008)

We show an efficient purification protocol in solid-state qubits by replacing the usual bilateral controlled-NOT gate by the bilateral *i*SWAP gate. We also show that this replacement can be applied to breeding and hashing protocols, which are useful for quantum state purification. These replacements reduce the number of fragile and cumbersome two-qubit operations, making more feasible quantum-information processing with solid-state qubits. As examples, we also present quantitative analyses for the required time to perform state purification using either superconducting or semiconducting qubits.

DOI: [10.1103/PhysRevA.78.062313](https://doi.org/10.1103/PhysRevA.78.062313)

PACS number(s): 03.67.Lx, 03.67.Ac, 85.25.Cp

I. INTRODUCTION

Quantum communications, such as quantum teleportation [1] and secure quantum cryptography [2], between two parties (Alice and Bob), require that qubits in highly entangled states, such as Bell states, be shared between the parties. The entanglement purification protocols proposed by Bennett *et al.* [3] and Deutsch *et al.* [4] are therefore not only important contributions to the theory of quantum information, but also essential ingredients to applications such as quantum communications. Starting from partially entangled states, these protocols distill near-maximally entangled states shared by distant parties. More specifically, in such a purification protocol, multiple pairs of qubits in impure entangled states are initially supplied, from which purified pairs are then obtained after sacrificing some of the impure pairs.

In each step of an entanglement purification protocol, local quantum computers have to carry out several single-qubit rotations and two-qubit operations on the local qubits at the sites of Alice and Bob, respectively. In particular, controlled-NOT (CNOT) gates play a major role in these purification protocols (as well as in other fields of quantum information and computation). In purification protocols [3,4], Alice and Bob repeat a process in which, after choosing two shared entangled pairs in mixed states, they bilaterally apply CNOT gates to their two local qubits that belong to the shared pairs, and measure one of the pairs. If the measured qubits are in either the $|00\rangle$ or $|11\rangle$ state, then the unmeasured pair is forwarded to the next step; otherwise the unmeasured pair is discarded. In the more efficient Deutsch *et al.* protocol [4], tens of such repetitions are needed, which means that a corresponding number of CNOT gates needs to be employed, and they should work with very low error rate.

For most solid-state qubits, two-qubit interactions are quite delicate and are difficult to control without error and decoherence. As such, creating quantum algorithms that employ *fewer* two-qubit operations is important to the successful construction of solid-state quantum-information processors. This optimization of the algorithmic aspects demands a

closer inspection of the omnipresent CNOT gate, a standard two-qubit gate. The CNOT gate is most conveniently generated from Ising interactions. However, general solid-state interqubit interactions are not of the Ising type. Instead, they are often in the form of the Heisenberg exchange (e.g., as in electrically tuned quantum dots) or *XY* model [e.g., cavity-coupled semiconducting quantum dots (QDs) [5] or superconducting Josephson qubits [6]]. In general, when a CNOT gate is constructed using the Heisenberg exchange or the *XY* interaction, *at least twice* the number of two-qubit interactions have to be invoked with complicated pulse sequences. A key question is thus whether it is possible to devise quantum algorithms that take better advantage of these two particular qubit interactions, instead of relying exclusively on the standard but cumbersome CNOT gate.

A further incentive to study *XY*-model-based quantum algorithms lies in the recent advances in cavity coupling of Josephson superconducting qubits (see, e.g., [6–9]) and cavity quantum electrodynamics (QED) of Josephson qubits, because it is relatively easy to reach the strongly interacting regime for these systems. Since cavity QED plays an important role for information exchange between static and flying qubits in quantum-communication networks, and the effective interaction between cavity-coupled qubits is described by the *XY* model, the development of *XY*-model-based quantum algorithms would pave the way for an easier integration of solid-state qubits into a quantum-communication network.

In this paper we study how to *efficiently* build entanglement purification protocols based on a two-qubit gate that can be easily generated by the *XY* interaction. It is important to note that it is relatively easy to generate the *i*SWAP gate in the *XY* model. Indeed, the *i*SWAP gate is a universal gate in quantum computation, and the CNOT gate is built using *two* *i*SWAP gates *and* several single-qubit gates [10]. Here, we discuss how to reduce the use of *i*SWAP gates in purification protocols, and we show that the bilateral CNOT gate (BCNOT) used in entanglement purification protocols can be replaced by a bilateral *i*SWAP gate (BiSWAP). For solid-state qubits with *XY* interqubit interactions, this change of gates leads to a significant simplification of each step of the entanglement

purification protocol, and to a much higher robustness of the protocol. Furthermore, purification protocols are often followed by hashing or breeding protocols. Here we show that the bilateral CNOT gates in the hashing or breeding protocols can also be replaced by bilateral iSWAP gates. In addition, we also discuss a purification protocol using $\sqrt{\text{SWAP}}$ gates, which are the basic and universal operations for qubits that are coupled via Heisenberg exchange interactions.

The rest of the paper is organized as follows. In Sec. II, we formulate the iSWAP gate from the XY model Hamiltonian and the $\sqrt{\text{SWAP}}$ gate in the Heisenberg model. In Sec. III, we show a purification protocol based on the iSWAP gate and discuss the effect of gate errors. In Sec. IV, we discuss the replacement of CNOT gates by iSWAP gates in the hashing and breeding protocols. In Sec. V, we show an effective method of generating the four Bell states based on the iSWAP gate. In Sec. VI, we give four examples of the application of the present method. Sections VII and VIII present discussions and a summary. In the Appendix, we summarize the derivation of the XY interaction from a general qubit-cavity Hamiltonian. Let us note that we do not assume any particular method for distributing entangled qubits. In the following discussions, noisy entanglement is taken as a resource.

II. ISWAP GATE IN THE XY MODEL AND THE $\sqrt{\text{SWAP}}$ GATE IN THE HEISENBERG MODEL

In this section we formulate the iSWAP gate from the XY model, and estimate the time required to obtain a conventional CNOT gate using an iSWAP gate. We also consider the case of the $\sqrt{\text{SWAP}}$ gate from the Heisenberg model.

The Hamiltonian of a coupled qubit-cavity system is typically given by the Jaynes-Cummings Hamiltonian, representing a linear interaction between a two-level system and a bosonic degree of freedom for the cavity, such as photons. When two qubits are coupled to the same cavity mode, the effective two-qubit interaction is described by the XY model. A derivation of the XY interaction from the Jaynes-Cummings Hamiltonian is given in the Appendix.

The XY model is expressed by the Hamiltonian $H_{xy} = \sum_{i<j} H_{xy}^{(ij)}$ with

$$H_{xy}^{(ij)} = J_{ij}(\sigma_i^x \sigma_j^x + \sigma_i^y \sigma_j^y), \quad (1)$$

where σ_i^α ($\alpha=x, y, z$) are the Pauli matrices acting on the i th qubit with basis $|0\rangle = |\downarrow\rangle$ and $|1\rangle = |\uparrow\rangle$. Two-qubit operations produced by $H_{xy}^{(12)}$ acting on qubits 1 and 2 can thus be expressed as

$$U_{xy}^{(12)}(t) = e^{-itH_{xy}^{(12)}} = \begin{pmatrix} 1 & 0 & 0 & 0 \\ 0 & \cos 2Jt & -i \sin 2Jt & 0 \\ 0 & -i \sin 2Jt & \cos 2Jt & 0 \\ 0 & 0 & 0 & 1 \end{pmatrix} \quad (2)$$

with $J=J_{12}$. Note that the iSWAP gate is obtained when $t = \tau_{\text{iSWAP}} \equiv \pi/(4J)$ such that

$$\begin{aligned} |00\rangle &\rightarrow |00\rangle, & |11\rangle &\rightarrow |11\rangle, \\ |01\rangle &\rightarrow -i|10\rangle, & |10\rangle &\rightarrow -i|01\rangle. \end{aligned} \quad (3)$$

The conventional CNOT gate is constructed with two iSWAP gates and four single-qubit rotations:

$$U_{\text{CNOT}}^{(12)} = e^{-i(\pi/4)\sigma_1^z} e^{i(\pi/4)\sigma_2^x} e^{i(\pi/4)\sigma_2^z} U_{\text{iSWAP}} e^{i(\pi/4)\sigma_1^x} \times U_{\text{iSWAP}} e^{i(\pi/4)\sigma_2^z}, \quad (4)$$

with [10]

$$U_{\text{iSWAP}} \equiv U_{xy}^{(12)}(t = \tau_{\text{iSWAP}}). \quad (5)$$

Thus, in order to produce a single CNOT operation, we have to precisely control two two-qubit operations and four single-qubit rotations. If we denote a single-qubit frequency as ω_{rot} , the time for a single-qubit rotation is typically $\tau_{\text{rot}} = \pi/(4\omega_{\text{rot}})$. The time to implement a CNOT gate is thus

$$\tau_{\text{CNOT}} \approx 4\tau_{\text{rot}} + 2\tau_{\text{iSWAP}} = \left(\frac{1}{\omega_{\text{rot}}} + \frac{2}{J} \right) \pi. \quad (6)$$

In this paper, we also study qubits whose interaction Hamiltonian is an isotropic Heisenberg form, written as $H_H = \sum_{i<j} H_H^{(ij)}$ with

$$H_H^{(ij)} = J_H(\sigma_i^x \sigma_j^x + \sigma_i^y \sigma_j^y + \sigma_i^z \sigma_j^z). \quad (7)$$

In this case, the typical two-qubit gate operation is $\sqrt{\text{SWAP}}$, which is defined by [11]

$$U_{\sqrt{\text{SWAP}}} \equiv U_H^{(12)}(t = \tau_{\sqrt{\text{SWAP}}}). \quad (8)$$

The CNOT gate is expressed by $U_{\text{CNOT}}^{(12)} = e^{-i(\pi/4)\sigma_2^y} U_{\text{CPF}}^{(12)} e^{i(\pi/4)\sigma_2^y}$, where the controlled phase flip (CPF) gate is obtained by

$$U_{\text{CPF}}^{(12)} = e^{-i(\pi/2)\sigma_1^z} e^{i(\pi/4)\sigma_1^z} e^{-i(\pi/4)\sigma_2^z} U_{\sqrt{\text{SWAP}}} e^{-i(\pi/2)\sigma_2^z} U_{\sqrt{\text{SWAP}}}. \quad (9)$$

Thus, the time to implement a CNOT gate becomes

$$\tau_{\text{CNOT}}^H \approx 3\tau_{\text{rot}} + 2\tau_{\sqrt{\text{SWAP}}}. \quad (10)$$

III. SIMPLIFICATION OF THE PURIFICATION PROTOCOL

A. State purification using iSWAP gates

In this section we show that the two purification protocols proposed by Bennett *et al.* [3] and Deutsch *et al.* [4] can be recast using the iSWAP gate instead of the CNOT gate (Fig. 1). The initially supplied entangled pairs of qubits are assumed to be in a mixed state ρ . The purification protocol proceeds recursively by choosing two entangled pairs, applying a bilateral CNOT gate, and measuring one of the pairs (called target qubits). The application of the bilateral CNOT gate to two pairs (Fig. 1), ρ_S (source pair) and ρ_T (target pair), is described by

$$\rho_S \otimes \rho_T \rightarrow U_{\text{BCNOT}}(\rho_S \otimes \rho_T) U_{\text{BCNOT}}^\dagger, \quad (11)$$

where U_{BCNOT} indicates that Alice and Bob bilaterally operate the CNOT gate on their local qubits that belong to ρ_S and ρ_T . Here we use the four Bell basis states

$$\Phi^\pm = (|\uparrow\uparrow\rangle \pm |\downarrow\downarrow\rangle)/\sqrt{2}, \quad \Psi^\pm = (|\uparrow\downarrow\rangle \pm |\downarrow\uparrow\rangle)/\sqrt{2}. \quad (12)$$

Then, as an example, the bilateral CNOT gate works like this:

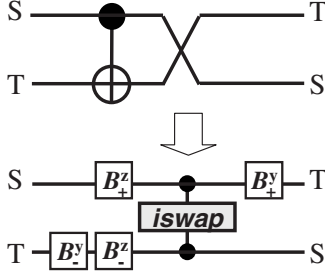


FIG. 1. Replacement of a bilateral CNOT (BCNOT) gate by a bilateral iSWAP (BiSWAP) gate. This figure shows the protocol for one of the parties. The complete protocol is achieved by the execution of the same operation at both ends. Here, we define bilateral single-qubit $\pm\pi/2$ rotations for Alice and Bob about the x , y , and z axes like those in Ref. [3], denoted by B_{\pm}^x , B_{\pm}^y , and B_{\pm}^z , respectively.

$$U_{\text{BCNOT}} \Psi_S^+ \Phi_T^- = \Psi_S^- \Psi_T^- \quad (13)$$

between a source pair

$$\Psi_S^+ = (|\uparrow_S^A \uparrow_S^B\rangle + |\downarrow_S^A \downarrow_S^B\rangle) / \sqrt{2} \quad (14)$$

and a target pair

$$\Phi_T^- = (|\uparrow_T^A \uparrow_T^B\rangle - |\downarrow_T^A \downarrow_T^B\rangle) / \sqrt{2}, \quad (15)$$

where $|\uparrow_{\eta}^A\rangle$ and $|\downarrow_{\eta}^A\rangle$ denote qubits that belong to Alice, and $|\downarrow_{\eta}^B\rangle$ and $|\downarrow_{\eta}^A\rangle$ indicate those that belong to Bob ($\eta=S, T$).

Below we show that the conventional bilateral CNOT gate can be replaced by the bilateral iSWAP gate together with a few single-qubit rotations (see Fig. 2). First we introduce the gates involved. The BiSWAP gate is defined as an application of the iSWAP gate at both locations to a pair of entangled qubits depicted in Fig. 1 (we call one pair the source and the other the target, as in Refs. [3,4]). The iSWAP gate can be expressed as

$$U_{\text{iSWAP}} = |\uparrow_S \uparrow_T\rangle \langle \uparrow_S \uparrow_T| + |\downarrow_S \downarrow_T\rangle \langle \downarrow_S \downarrow_T| - i|\uparrow_S \downarrow_T\rangle \langle \downarrow_S \uparrow_T| - i|\downarrow_S \uparrow_T\rangle \langle \uparrow_S \downarrow_T|, \quad (16)$$

by using Eqs. (2) and (5). Here is an example of the BiSWAP gate:

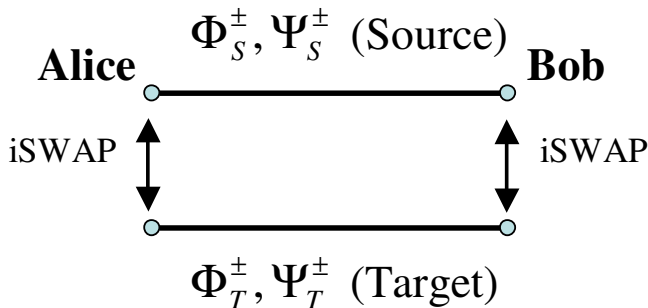


FIG. 2. (Color online) Bilateral iSWAP (BiSWAP) gate. The iSWAP gates are bilaterally applied by Alice and Bob.

TABLE I. Bilateral rotations. Note that, except for the coefficient $\pm i$, for the B_{\pm}^x mapping, $\Phi^+ \leftrightarrow \Psi^+$ are exchanged. For the B_{\pm}^y mapping, the states $\Phi^- \leftrightarrow \Psi^+$ are exchanged. Finally, for B_{\pm}^z mapping, the states $\Phi^+ \leftrightarrow \Phi^-$ are exchanged. The singlet state Ψ^- is unchanged.

	Φ^+	Φ^-	Ψ^+	Ψ^-
B_{\pm}^x	$\pm i\Psi^+$	Φ^-	$\pm i\Phi^+$	Ψ^-
B_{\pm}^y	Φ^+	$\mp\Psi^+$	$\pm\Phi^-$	Ψ^-
B_{\pm}^z	$\pm i\Phi^-$	$\pm i\Phi^+$	Ψ^+	Ψ^-

$$U_{\text{BiSWAP}} \Phi_S^- \Phi_T^{\pm} = |\uparrow_S \uparrow_T\rangle \langle \uparrow_T \uparrow_T| \mp |\downarrow_S \downarrow_S\rangle \langle \uparrow_T \uparrow_T| + |\uparrow_S \uparrow_S\rangle \langle \downarrow_T \downarrow_T| \mp |\downarrow_S \downarrow_S\rangle \langle \downarrow_T \downarrow_T| = \Phi_S^{\mp} \Phi_T^{\pm}. \quad (17)$$

Similarly to the BiSWAP gate, we also define bilateral single-qubit $\pm\pi/2$ rotations for Alice and Bob about the x , y , and z axes like those in Ref. [3], denoted by B_{\pm}^x , B_{\pm}^y , and B_{\pm}^z , respectively. For example (the complete logic table is given in Table I),

$$B_{S^+}^x \Psi_S^+ = e^{i\pi\sigma_A^x/4} e^{i\pi\sigma_B^x/4} (|\downarrow_S^A \uparrow_S^B\rangle + |\uparrow_S^A \downarrow_S^B\rangle) = i\Phi_S^+. \quad (18)$$

The key issue to replacing BCNOT gates by BiSWAP gates is how to convert the relationship between CNOT and iSWAP gates into a bilateral form. The basic relationship between the CNOT gate and the iSWAP gate can be derived by starting from the fundamental property that the iSWAP gate can be decomposed into a CNOT gate and a SWAP gate between qubits 1 and 2:

$$U_{\text{iSWAP}} = U_{\text{SWAP}} \text{diag}(1, -i, -i, 1). \quad (19)$$

Thus, the relationship between the CPF gate $U_{\text{CPF}} = \text{diag}(I, \sigma^z)$ (I is a unit 2×2 matrix) and the iSWAP gate can be described as

$$U_{\text{CPF}} = \text{diag}(1, -i, -i, 1) P_{1+} P_{2+} = U_{\text{SWAP}} U_{\text{iSWAP}} P_{1+} P_{2+}, \quad (20)$$

where $P_{1+} = e^{-i(\pi/4)\sigma_1^z} \otimes I$ and $P_{2+} = I \otimes e^{-i(\pi/4)\sigma_2^z}$ are $\pi/2$ rotations around the z axis on one of the qubits. Using $H_1 = H \otimes I$ and $H_2 = I \otimes H$ with the Hadamard matrix

$$H = \frac{1}{\sqrt{2}} \begin{pmatrix} 1 & 1 \\ 1 & -1 \end{pmatrix} \quad (21)$$

and the relation $U_{\text{CNOT}} = H_2 U_{\text{CPF}} H_2$, we have

$$U_{\text{SWAP}} U_{\text{CNOT}} = U_{\text{SWAP}} H_2 U_{\text{SWAP}} U_{\text{iSWAP}} P_{1+} P_{2+} H_2 = H_1 U_{\text{iSWAP}} P_{1+} P_{2+} H_2. \quad (22)$$

We construct a bilateral version of this equation. The basic strategy is to replace each qubit operation by a bilateral one, one by one. Note that we do not always have to replace each operation in Eq. (22) by the bilateral operation that exactly corresponds to the original unilateral operation. As long as the same effect can be obtained, we can instead use a simpler operation. Then, by observing the roles of each operation, we find the relation

TABLE II. Replacement of a BCNOT by a BiSWAP gate. Note that the initial state in the leftmost column is subject to four operations or steps described in the remaining four columns.

Initial state	Step (i) B_{T-}^y	Step (ii) $B_{S+}^z B_{T-}^z$	Step (iii) BiSWAP	Final step (iv) B_{S+}^y
$\Phi_S^+ \Phi_T^+$	$\Phi_S^+ \Phi_T^+$	$\Phi_S^- \Phi_T^-$	$\Phi_S^+ \Phi_T^+$	$\Phi_S^+ \Phi_T^+$
$\Phi_S^+ \Phi_T^-$	$\Phi_S^+ \Psi_T^+$	$i \Phi_S^- \Psi_T^+$	$\Psi_S^+ \Phi_T^-$	$\Phi_S^- \Phi_T^-$
$\Phi_S^+ \Psi_T^+$	$-\Phi_S^+ \Phi_T^-$	$-\Phi_S^- \Phi_T^+$	$-\Phi_S^- \Phi_T^+$	$\Psi_S^+ \Phi_T^+$
$\Phi_S^+ \Psi_T^-$	$\Phi_S^+ \Psi_T^-$	$i \Phi_S^- \Psi_T^-$	$\Psi_S^+ \Phi_T^-$	$\Psi_S^- \Phi_T^-$
$\Phi_S^- \Phi_T^+$	$\Phi_S^- \Phi_T^+$	$\Phi_S^+ \Phi_T^-$	$\Phi_S^+ \Phi_T^-$	$\Phi_S^+ \Phi_T^-$
$\Phi_S^- \Phi_T^-$	$\Phi_S^- \Psi_T^+$	$i \Phi_S^+ \Psi_T^+$	$\Psi_S^+ \Phi_T^+$	$\Phi_S^- \Phi_T^+$
$\Phi_S^- \Psi_T^+$	$-\Phi_S^- \Phi_T^-$	$-\Phi_S^+ \Phi_T^+$	$-\Phi_S^+ \Phi_T^+$	$\Psi_S^+ \Phi_T^-$
$\Phi_S^- \Psi_T^-$	$\Phi_S^- \Psi_T^-$	$i \Phi_S^+ \Psi_T^-$	$\Psi_S^+ \Phi_T^+$	$\Psi_S^- \Phi_T^+$
$\Psi_S^+ \Phi_T^+$	$\Psi_S^+ \Phi_T^+$	$-i \Psi_S^- \Phi_T^-$	$-\Phi_S^- \Psi_T^+$	$\Psi_S^+ \Psi_T^+$
$\Psi_S^+ \Phi_T^-$	$\Psi_S^+ \Psi_T^+$	$\Psi_S^+ \Psi_T^+$	$\Psi_S^- \Psi_T^-$	$\Psi_S^- \Psi_T^-$
$\Psi_S^+ \Psi_T^+$	$-\Psi_S^+ \Phi_T^-$	$i \Psi_S^- \Phi_T^+$	$\Phi_S^+ \Psi_T^+$	$\Phi_S^+ \Psi_T^+$
$\Psi_S^+ \Psi_T^-$	$\Psi_S^+ \Psi_T^-$	$\Psi_S^+ \Psi_T^-$	$\Psi_S^- \Psi_T^-$	$\Phi_S^- \Psi_T^-$
$\Psi_S^- \Phi_T^+$	$\Psi_S^- \Phi_T^+$	$-i \Psi_S^- \Phi_T^-$	$-\Phi_S^- \Psi_T^-$	$\Psi_S^+ \Psi_T^-$
$\Psi_S^- \Phi_T^-$	$\Psi_S^- \Psi_T^+$	$\Psi_S^- \Psi_T^+$	$\Psi_S^- \Psi_T^+$	$\Psi_S^- \Psi_T^+$
$\Psi_S^- \Psi_T^+$	$-\Psi_S^- \Phi_T^-$	$i \Psi_S^- \Phi_T^+$	$\Phi_S^+ \Psi_T^-$	$\Phi_S^+ \Psi_T^-$
$\Psi_S^- \Psi_T^-$	$\Psi_S^- \Psi_T^-$	$\Psi_S^- \Psi_T^-$	$\Psi_S^+ \Psi_T^+$	$\Phi_S^- \Psi_T^+$

$$U_{\text{BCNOT}} = U_{\text{BSWAP}} B_{S+}^y U_{\text{BiSWAP}} B_{S+}^z B_{T-}^z B_{T-}^y. \quad (23)$$

Here, we find that we can replace the Hadamard gates by B_{\pm}^y gates by just adjusting the coefficients of the wave functions in the four steps. This is the reason that here we introduce B_{-}^x , B_{-}^y , and B_{-}^z , in addition to B_{+}^x , B_{+}^y , and B_{+}^z from Ref. [3]. Of course, we can express the bilateral Hadamard gate conventionally using three single-qubit operations as $B_{+}^x B_{+}^z B_{+}^x$. However, the Hadamard gate by these three rotations should be avoided so that we can reduce the operation time. Also note that we do *not* need to carry out the SWAP gate in Eq. (23), because we only have to choose one of the qubits to be measured after the BiSWAP gate. Indeed, the SWAP gate is expressed mathematically by three CNOT gates; therefore, faithfully following Eq. (23) goes against our aim of reducing the number of gate operations. In the conventional purification process, after the BCNOT gate, the target qubits are measured and checked as to whether they are in $|\uparrow\uparrow\rangle$ or $|\downarrow\downarrow\rangle$. In the present case, where we use the iSWAP gate, we measure the source qubits instead of the target qubits and keep the target qubits for the next step, if the source qubits are in $|\uparrow\uparrow\rangle$ or $|\downarrow\downarrow\rangle$. Here, the SWAP process is irrelevant in this purification process.

The whole pulse sequence in Eq. (23) is described in Table II step by step. In step (i), the B_{-}^y mapping is applied only to the target qubits. In step (ii), the B_{+}^z mapping is applied to the source qubits, and the B_{-}^z mapping is applied to the target qubits. In step (iii), the BiSWAP gate is applied between the source pair and the target pair (Fig. 1). Finally, in step (iv), the B_{+}^y mapping is carried out on the source pair. Comparing the rightmost column with the expected results of the BCNOT gate, we can see that the sequence (23) is equivalent

to the BCNOT gate, including its coefficients. Because we can express U_{BCNOT} as

$$U_{\text{BCNOT}} = H_2 P_{1+} P_{2+} U_{\text{iSWAP}} H_1 U_{\text{SWAP}} \quad (24)$$

in the reversed order, we can also reverse the order of the operation by taking the Hermitian conjugate of U_{BCNOT} as

$$U_{\text{BCNOT}}^\dagger = B_{T+}^y B_{S+}^z B_{T-}^z U_{\text{BiSWAP}} B_{S-}^y U_{\text{BSWAP}}. \quad (25)$$

The Deutsch *et al.* protocol [4] is more efficient than the Bennett *et al.* protocol [3], because the former does not need a Werner state (see below) [12]. In the Deutsch *et al.* purification protocol, $\pm\pi/2$ rotations around the x axis should be applied before each BCNOT gate. Thus, in this protocol, we also have to apply the same $\pm\pi/2$ rotations around the x axis before the process shown in Table II. If we realize the Deutsch *et al.* protocol using the conventional CNOT gate Eq. (6), then the time needed for each process in the purification protocol is given by

$$\tau_{\text{puri}}^{\text{BCNOT}} \approx 5\tau_{\text{tot}} + 2\tau_{\text{iSWAP}}. \quad (26)$$

If we replace the CNOT part of the Deutsch *et al.* protocol by our method, we need three single-qubit rotations, B_{T-}^y in step (i), B_{S+}^z and B_{T-}^z in step (ii), and B_{S+}^y in step (iv), plus an iSWAP gate in step (iii). From Eq. (23) or (25), the time $\tau_{\text{puri}}^{\text{BiSWAP}}$ for this entire process in the purification using the BiSWAP gate is given by

$$\tau_{\text{puri}}^{\text{BiSWAP}} \approx 4\tau_{\text{tot}} + \tau_{\text{iSWAP}}. \quad (27)$$

Thus, the time advantage $\Delta\tau_{\text{puri}}^{\text{adv}}$ of our method is given by

$$\Delta\tau_{\text{puri}}^{\text{adv}} = \tau_{\text{puri}}^{\text{BCNOT}} - \tau_{\text{puri}}^{\text{BiSWAP}} \approx \tau_{\text{tot}} + \tau_{\text{iSWAP}}. \quad (28)$$

In the Bennett *et al.* purification protocol, the mixed-state density matrix is assumed to be in a diagonal form called the Werner state

$$\rho = A|\Phi^+\rangle\langle\Phi^+| + B|\Psi^-\rangle\langle\Psi^-| + C|\Psi^+\rangle\langle\Psi^+| + D|\Phi^-\rangle\langle\Phi^-| \quad (29)$$

with $A=F$ and $B=C=D=(1-F)/3$, where F is the fidelity with respect to Φ^+ . The simple form of the density matrix Eq. (29) also makes our replacement simpler. This is because, when $B=C=D$, the B_{\pm}^y mapping does not affect the coefficient of the Werner state and, moreover, the diagonal form makes the coefficients of the bilateral transformations irrelevant to the purification process. The result is shown in Table III. In this case, after applying the BiSWAP gate to the initial mixed state Eq. (29), we can apply either step (iia) involving $B_{S\pm}^x$, $B_{T\pm}^x$ rotations, or step (iib) involving $B_{S\pm}^x$, $B_{T\pm}^x$ rotations. Thus, in this case, the protocol needs only two steps.

Here we assume that, for step (iia) in Table III, the probability of finding Φ^+ is F (Φ^\pm can be exchanged into Φ^\mp by a unilateral π rotation around the z axis) and the probability of finding the other states is $(1-F)/3$. For step (iib) in Table III, the probability of finding the state Ψ^- is F (Ψ^\pm can be exchanged by Φ^\pm by a unilateral π rotation around the x axis) and those of other states are $(1-F)/3$. We do not discard the Φ^\pm elements when measuring the target qubits, and take Φ_S^- as the target purified state. Then, the probability that

TABLE III. Bennett *et al.* [3] purification process for entangled states. Note that the initial state in the first column is subject to the steps shown in the following three columns. After applying a BiSWAP gate in step (i), the purification process requires applying either the step (iia) or the step (iib), but not both. The ‘‘Test result’’ columns provide terms that are used to compute fidelities shown in Eq. (30).

Initial state	Step (i) BiSWAP	step (iia) $B_{S\pm}^x B_{T\pm}^x$	Test result	Step (iib) $B_{S\pm}^y B_{T\pm}^y$	Test result
$\Phi_S^+ \Phi_T^+$	$\Phi_S^- \Phi_T^-$	$\Phi_S^- \Phi_T^-$	F^2	$\Psi_S^+ \Psi_T^+$	
$\Phi_S^+ \Phi_T^-$	$\Phi_S^+ \Phi_T^-$	$\Psi_S^+ \Phi_T^-$	$F \left(\frac{1-F}{3} \right)$	$\Phi_S^+ \Psi_T^+$	
$\Phi_S^+ \Psi_T^+$	$-i \Psi_S^+ \Phi_T^+$	$-i \Phi_S^+ \Psi_T^+$		$-i \Phi_S^- \Phi_T^+$	$\left(\frac{1-F}{3} \right)^2$
$\Phi_S^+ \Psi_T^-$	$-i \Psi_S^- \Phi_T^+$	$-i \Psi_S^- \Psi_T^+$		$-i \Psi_S^- \Phi_T^+$	$F \left(\frac{1-F}{3} \right)$
$\Phi_S^- \Phi_T^+$	$\Phi_S^- \Phi_T^+$	$\Phi_S^- \Psi_T^+$		$\Psi_S^+ \Phi_T^+$	$\left(\frac{1-F}{3} \right)^2$
$\Phi_S^- \Phi_T^-$	$\Phi_S^+ \Phi_T^+$	$\Psi_S^+ \Psi_T^+$		$\Phi_S^+ \Phi_T^+$	$\left(\frac{1-F}{3} \right)^2$
$\Phi_S^- \Psi_T^+$	$-i \Psi_S^+ \Phi_T^-$	$-i \Phi_S^+ \Phi_T^-$	$\left(\frac{1-F}{3} \right)^2$	$-i \Phi_S^- \Psi_T^+$	
$\Phi_S^- \Psi_T^-$	$-i \Psi_S^- \Phi_T^-$	$-i \Psi_S^- \Phi_T^-$	$\left(\frac{1-F}{3} \right)^2$	$-i \Psi_S^- \Psi_T^+$	
$\Psi_S^+ \Phi_T^+$	$-i \Phi_S^+ \Psi_T^+$	$-i \Psi_S^+ \Phi_T^+$	$F \left(\frac{1-F}{3} \right)$	$-i \Phi_S^+ \Phi_T^-$	$\left(\frac{1-F}{3} \right)^2$
$\Psi_S^+ \Phi_T^-$	$-i \Phi_S^- \Psi_T^+$	$-i \Phi_S^- \Phi_T^+$	$\left(\frac{1-F}{3} \right)^2$	$-i \Psi_S^+ \Phi_T^-$	$\left(\frac{1-F}{3} \right)^2$
$\Psi_S^+ \Psi_T^\pm$	$\Psi_S^- \Psi_T^-$	Discarded		Discarded	
$\Psi_S^- \Phi_T^\pm$	$-i \Phi_S^\pm \Psi_T^-$	Discarded		Discarded	
$\Psi_S^- \Psi_T^+$	$\Psi_S^- \Psi_T^+$	$\Psi_S^- \Phi_T^+$	$\left(\frac{1-F}{3} \right)^2$	$\Psi_S^- \Phi_T^-$	$F \left(\frac{1-F}{3} \right)$
$\Psi_S^- \Psi_T^-$	$\Psi_S^+ \Psi_T^+$	$\Phi_S^+ \Phi_T^+$	$\left(\frac{1-F}{3} \right)^2$	$\Phi_S^- \Phi_T^-$	F^2

the source qubits are in Φ_S^- after this purification process, is exactly the same as that from the Bennett *et al.* protocol [3]:

$$F' = \frac{F^2 + \left(\frac{1-F}{3} \right)^2}{F^2 + 2F \left(\frac{1-F}{3} \right) + 5 \left(\frac{1-F}{3} \right)^2}. \quad (30)$$

The fidelity of the target state is improved ($F' > F$) when $1/2 < F < 1$. Thus, we can show that the CNOT gate, which requires *two* processes of qubit-qubit interactions, can be replaced by *one* qubit-qubit interaction. This is a more efficient purification protocol.

B. Effect of errors

Here we check the effect of errors in the Bennett purification process shown in Table III. We assume that the XY interaction has a probable pulse error ϵ in controlling the interaction time as

$$2Jt = \pi/2 + \epsilon \quad (31)$$

($\epsilon \ll 1$) in Eq. (2). Then, for both columns (iia) and (iib) in Table III, we have the relation

$$F' = \frac{k_1^2 F^2 + k_3 \left(\frac{1-F}{3} \right)^2}{k_1 F^2 + 2F \left(\frac{1-F}{3} \right) + (5+k_2) \left(\frac{1-F}{3} \right)^2}, \quad (32)$$

where k_1 , k_2 , and k_3 are given, in second order on the error ϵ , by

$$k_1 = (1 + \cos 2\epsilon)/2 \sim (1 - \epsilon^2),$$

$$k_2 = (1 - \cos 2\epsilon)/2 \sim \epsilon^2,$$

$$k_3 = 1 + k_2 + \sin^2(2\epsilon)/4 \sim (1 + 2\epsilon^2). \quad (33)$$

From these equations, the original condition $F > 1/2$ to obtain the relation $F' > F$ is changed to $F > 1/2 + 3\epsilon^2$, to order ϵ^2 . Thus, if there is a pulse error, the initial fidelity for the purification process should be correspondingly increased.

C. Purification using $\sqrt{\text{SWAP}}$ gates

In the case of the Heisenberg interaction [16], we cannot directly replace the CNOT gate by a $\sqrt{\text{SWAP}}$ gate in the purification protocol. This is because the $\sqrt{\text{SWAP}}$ operation has off-diagonal matrix elements and mixes Bell states. Thus, for the Deutsch *et al.* purification protocol, we had better use the CNOT gate based on the two $\sqrt{\text{SWAP}}$ gates in the conventional way [Eq. (9)]. However, for the Bennett *et al.* protocol, we can slightly reduce the number of operations. For the Bennett case, we can use the CPF gate plus the B_{\pm}^y operation. The CPF gate transforms

$$\Phi^p \Phi^q \rightarrow \Phi^p \Phi^q, \quad (34)$$

$$\Psi^p \Psi^q \rightarrow -\Psi^{-p} \Phi^{-q}, \quad (35)$$

$$\Phi^p \Psi^q \rightarrow \Phi^{-p} \Psi^q, \quad (36)$$

$$\Psi^p \Phi^q \rightarrow \Psi^{-p} \Phi^{-q}, \quad (37)$$

where $p = \pm$, $q = \pm$. By combining the CPF gate with B_{\pm}^y , we can obtain the same equation as Eq. (30) for the Φ^+ state. In this case, the advantage is just the time τ_{rot} to perform a single-qubit rotation.

IV. REPLACEMENT OF BCNOT BY BISWAP GATE IN HASHING AND BREEDING PROTOCOL

The replacement of a BCNOT by a BiSWAP gate shown in the previous section can also be applied to more general

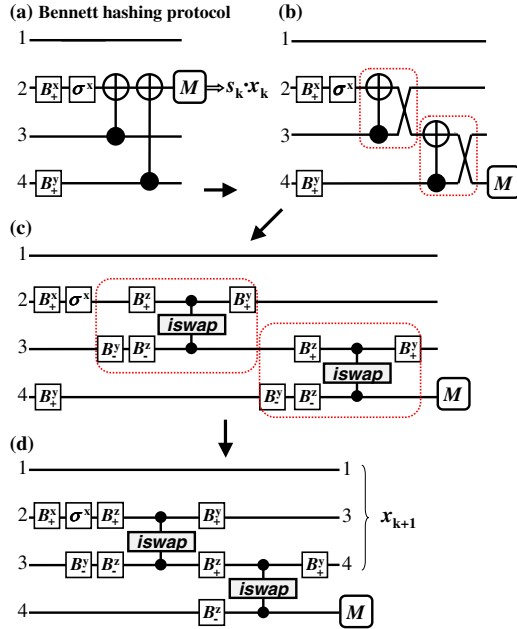


FIG. 3. (Color online) Replacement of a BCNOT gate by a BiSWAP gate in the hashing protocol. This figure shows the protocol for one of the parties. The complete protocol is achieved by executing the same operation at both ends. M denotes measurement.

cases where the BCNOT gate is used. Indeed, the BCNOT gate can be automatically replaced with the BiSWAP by the following procedure, using Eq. (23) or Eq. (25). This replacement process is more transparent and more formal than the purification process in the previous section. The procedure of replacement is as follows:

- (i) Apply a SWAP gate just after each BCNOT gate.
- (ii) Replace a BCNOT gate with a BiSWAP gate by Eq. (23) or Eq. (25).
- (iii) Contract a series of B_{\pm}^x , B_{\pm}^y , B_{\pm}^z and other single-qubit rotations to reduce the number of gate operations.

In the following two sections, we apply this method to the hashing and breeding protocols proposed by Bennett *et al.* [3]. Note that the process (i) does not mean that an additional SWAP gate is needed. That is, we can perform the numbering of output qubits without adding real gates.

A. Hashing using iSWAP gates

The hashing protocol proposed by Bennett *et al.* [3] is based on a one-way communication from Alice to Bob [see Fig. 3(a)]. In Fig. 3, σ^x , σ^y , and σ^z express unilateral π rotations of one particle. A sequence of unknown impure pairs, such as $\Psi^-\Phi^+\Phi^-\dots$ is regarded as a bit string 110010... by the definition

$$\Phi^+ = 00, \quad \Psi^+ = 10, \quad \Phi^- = 01, \quad \Psi^- = 11. \quad (38)$$

At the k th round of the hashing protocol for an initial set of n impure pairs, Alice first sends Bob a random $2(n-k)$ -bit string $s_k \in \{00, 11, 01, 10\}$ for the unknown $(n-k)$ impure pairs x_k . Depending on the value of s_k , gate operations for each pair are carried out following Fig. 3(a). Then, the parity of this random bit string is obtained by the measurement.

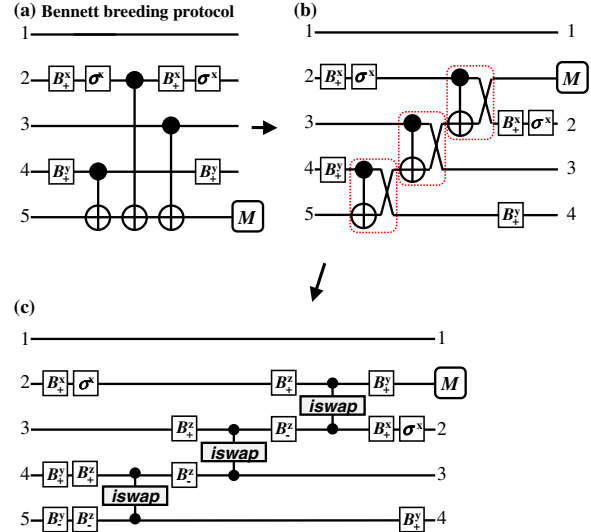


FIG. 4. (Color online) Replacement of a BCNOT gate by a BiSWAP gate in the breeding protocol. This figure shows the protocol for one of the parties. The complete protocol is achieved by executing the same operation at both ends.

Depending on the parity, the probability of the impure pair is reduced and we can increase the purity of the resulting states.

When we apply this hashing protocol by a local quantum computer, at least four qubits are required for the local quantum computer. We can simplify the hashing process after the purification, by using the BiSWAP gate as follows. We can replace each BCNOT gate by a BiSWAP gate, one by one, as shown in Figs. 3(b)–3(d). In Fig. 3(b), we first change the protocol such that a SWAP gate follows a CNOT gate. In Fig. 3(c), a CNOT gate plus a SWAP gate is replaced by an iSWAP gate as shown in Fig. 1 and Eq. (23).

B. Breeding protocol using iSWAP gates

Here we show an effective way of carrying out the breeding protocol proposed by Bennett *et al.* [3] [Fig. 4(a)]. The difference between the breeding and the hashing protocols is that, in the former case, Alice and Bob purify a sequence of impure states using a pool of initially prepared pure states, and the impure pairs do not have to be measured. Thus, the number of candidates of the impure set x is reduced by 1/2 for each breeding process, although pure Bell states should be prepared in advance. In this breeding protocol, three CNOT gates are required per each single process. Thus, we need three iSWAP gates in order to replace CNOT gates by iSWAP gates. Figures 4(b) and 4(c) show the process of this replacement. First, a SWAP gate is inserted just after each CNOT gate [Fig. 4(b)]. Note that, in Fig. 4(b), we have replaced each two original CNOT gates by an iSWAP gate between nearest qubits. Next, each pair of CNOT and SWAP gates is replaced by a set of iSWAP gates and single-qubit rotations, according to Eq. (23). Finally, a series of B^y gates is contracted. Then we obtain the breeding protocol using iSWAP gates.

V. GENERATION OF BELL STATES

In the previous sections, we have assumed that Bell states are initially prepared and distributed to two parties. Here,

TABLE IV. Summary of the operation time improvements by using our proposed method. For $\tau_{\text{puri}}^{\text{BiSWAP}}$ see Eq. (27), for $\tau_{\text{Bell}}^{\text{iSWAP}}$, see Eq. (45), and for $\tau_{\text{Bell}}^{\text{SWAP}}$ see Eq. (48).

New operation time	Previous operation time	Time advantage
$\tau_{\text{puri}}^{\text{BiSWAP}} \approx 4\tau_{\text{rot}} + \tau_{\text{iSWAP}}$	$\tau_{\text{puri}}^{\text{BCNOT}} \approx 5\tau_{\text{rot}} + 2\tau_{\text{iSWAP}}$	$\tau_{\text{rot}} + \tau_{\text{iSWAP}}$
$\tau_{\text{Bell}}^{\text{iSWAP}} \approx 2\tau_{\text{rot}} + \tau_{\text{iSWAP}}$	$\tau_{\text{Bell}}^{\text{CNOT}} \approx 5\tau_{\text{rot}} + 2\tau_{\text{iSWAP}}$	$3\tau_{\text{rot}} + \tau_{\text{iSWAP}}$
$\tau_{\text{Bell}}^{\text{SWAP}} \approx 3\tau_{\text{rot}} + \tau_{\text{SWAP}}$	$\tau_{\text{Bell}}^{\text{CNOT}} \approx 4\tau_{\text{rot}} + 2\tau_{\text{SWAP}}$	$\tau_{\text{rot}} + \tau_{\text{SWAP}}$

assuming a situation that four Bell states should be generated by local quantum computers, we show an effective way of generating the four Bell states by an iSWAP gate and a $\sqrt{\text{SWAP}}$ gate. Conventionally, the Bell states are produced by applying the CNOT gate to product states such as

$$U_{\text{CNOT}}(|0\rangle_S + |1\rangle_S)|1\rangle_T = |01\rangle + |10\rangle. \quad (39)$$

When we use the iSWAP gate, Bell states can be generated by turning on one iSWAP gate with $\pm\pi/2$ rotations around the y axis [13] as follows:

$$e^{i(\pi/4)\sigma_2^y} U_{\text{iSWAP}}^{(12)} |+\rangle_{y1} |+\rangle_{y2} = |0\rangle_1 |1\rangle_2 + |1\rangle_1 |0\rangle_2, \quad (40)$$

$$e^{-i(\pi/4)\sigma_2^y} U_{\text{iSWAP}}^{(12)} |+\rangle_{y1} |+\rangle_{y2} = |0\rangle_1 |0\rangle_2 - |1\rangle_1 |1\rangle_2, \quad (41)$$

$$e^{i(\pi/4)\sigma_2^y} U_{\text{iSWAP}}^{(12)} |+\rangle_{y1} |-\rangle_{y2} = |0\rangle_1 |0\rangle_2 + |1\rangle_1 |1\rangle_2, \quad (42)$$

$$e^{-i(\pi/4)\sigma_2^y} U_{\text{iSWAP}}^{(12)} |+\rangle_{y1} |-\rangle_{y2} = -|0\rangle_1 |1\rangle_2 + |1\rangle_1 |0\rangle_2, \quad (43)$$

where $|\pm\rangle_y \equiv |0\rangle \pm i|1\rangle$ are eigenstates of σ^y and $U_{\text{iSWAP}} |-\rangle_{y1} |-\rangle_{y2}$ is a two-qubit cluster state shown in Refs. [13,14]. If we start from a product state $|00\rangle$, we need two rotations and one iSWAP gate to create four Bell states. In these cases, we conventionally need an operation time

$$\tau_{\text{Bell}}^{\text{CNOT}} \approx 5\tau_{\text{rot}} + 2\tau_{\text{iSWAP}}. \quad (44)$$

In the present method, we just need

$$\tau_{\text{Bell}}^{\text{iSWAP}} \approx 2\tau_{\text{rot}} + \tau_{\text{iSWAP}}. \quad (45)$$

Therefore, the time advantage is given by

$$\Delta\tau_{\text{Bell}}^{\text{adv iSWAP}} = \tau_{\text{Bell}}^{\text{CNOT}} - \tau_{\text{Bell}}^{\text{iSWAP}} \approx 3\tau_{\text{rot}} + \tau_{\text{iSWAP}}. \quad (46)$$

Thus, we can reduce the time $\Delta\tau_{\text{Bell}}^{\text{adv iSWAP}}$ for generating the Bell states. Similarly, we can produce the Bell states by a single use of $\sqrt{\text{SWAP}}$. Because of the relation

$$U_{\sqrt{\text{SWAP}}} |+\rangle_1 |-\rangle_2 = |0\rangle_1 \{|0\rangle_2 - i|1\rangle_2\} + i|1\rangle_1 \{|0\rangle_2 + i|1\rangle_2\}, \quad (47)$$

if we apply $e^{\pm i(\pi/4)\sigma_1^z}$ on qubit 1 and $e^{i(\pi/4)\sigma_2^x} e^{i(\pi/4)\sigma_2^y}$ on qubit 2, we obtain Φ^\pm . If we apply $e^{\pm i(\pi/4)\sigma_1^z}$ on qubit 1 and $e^{-i(\pi/4)\sigma_2^x} e^{i(\pi/4)\sigma_2^y}$ on qubit 2, we obtain Ψ^\pm . In these cases, we can reduce the time to

$$\tau_{\text{Bell}}^{\text{SWAP}} \approx 3\tau_{\text{rot}} + \tau_{\text{SWAP}}, \quad (48)$$

compared with the conventionally necessary time

$$\tau_{\text{Bell}}^{\text{CNOT}} \approx 4\tau_{\text{rot}} + 2\tau_{\text{SWAP}}. \quad (49)$$

Thus, the time advantage now becomes

$$\Delta\tau_{\text{Bell}}^{\text{adv SWAP}} = \tau_{\text{Bell}}^{\text{CNOT}} - \tau_{\text{Bell}}^{\text{SWAP}} \approx \tau_{\text{rot}} + \tau_{\text{SWAP}}. \quad (50)$$

Table IV summarizes the operation time advantage discussed in this paper.

VI. APPLICATION OF THE iSWAP PURIFICATION PROCESS

In this section we quantitatively examine several examples using the XY interaction and compare our method with the conventional ones in the literature, which are based on the CNOT gate.

(1) Imamoglu *et al.* [5] proposed a quantum computing architecture where localized electron spins in QDs are qubits, and they interact with each other via the coupling to the vacuum field of a common microcavity. In this case, the qubit-qubit interaction mediated by the cavity photon is expressed by the XY model with $J=g^2/\Delta$, where Δ is the two-photon detuning and g is an effective two-photon coupling coefficient for the spin qubits. Based on the parameters in the proposal, it takes about 30 ps per each iSWAP gate and 10 ps per each single-qubit rotation, so that it takes ~ 100 ps for the CPF gate operation. If we assume that two rotations should be added to the CPF gate in order to obtain the CNOT gate, it takes about 120 ps for the CNOT operation. Now if we replace the CNOT gate by the iSWAP gate, we need 60 ps in total from Eq. (27). Thus the operation time of our method is about half that of the conventional method.

(2) When two superconducting charge qubits interact with each other via capacitive coupling to a common superconducting coplanar resonator, the resulting effective interqubit interaction is also described by the XY model [7]. Using $g/\Delta=0.1$, $g/(2\pi)=200$ MHz, $\Delta/(2\pi)=2$ GHz, we have $J/(2\pi)=20$ MHz and $\tau_{\text{iSWAP}}=6.25$ ns. With $\omega_{\text{rot}}/(2\pi)\sim 1$ GHz, we have $\tau_{\text{rot}}\sim 125$ ps. Thus, we have $\tau_{\text{puri}}^{\text{BCNOT}}\sim 13.1$ ns and $\tau_{\text{puri}}^{\text{BiSWAP}}\sim 6.75$ ns for a dephasing time of about 500 ns. This means that our purification method is about twice as fast as the conventional one for entanglement purification. We can also apply our method to purify flux qubits connected by a common LC circuit data bus [15].

In the cases where multiple qubits are connected by a common cavity field or data bus, when we want to purify qubits by the method mentioned above, we can choose only one two-qubit pair at a time, since we cannot control more than three qubits simultaneously.

(3) Our method can be applied to purify solid-state qubits with XY interactions, with or without cavity photons. Figure

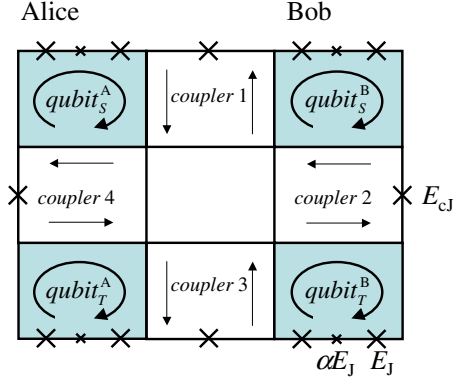


FIG. 5. (Color online) Four flux qubits coupled by four couplers. Initially, the upper two qubits (source qubits) and the lower two qubits (target qubits) are entangled, respectively, forming mixed states. After the purification process, the upper source qubits are σ^z measured.

5 shows four three-junction superconducting flux qubits, coupled to their neighbors via single Josephson junction couplers. This setup is obtained by extending the setup shown in Refs. [17–21]. We take $E_{cJ} > E_J$ and $0.5 < \alpha < 1$ such that only the ground state of the four couplers (classical region) is involved in the coupling process, and each of the three-Josephson-junction loops constitutes a flux qubit. Here we can consider the purification process of an entangled state between qubit_T^A and qubit_T^B using qubit_S^A and qubit_S^B , by controlling the four couplers that exist between each pair of neighboring qubits. If we use experimental values $J/(2\pi) \sim 25$ MHz [17] and a single qubit frequency of 1 GHz [22], the gate times are $\tau_{\text{SWAP}} \sim 5$ ns and $\tau_{\text{rot}} \sim 125$ ps. Thus, $\tau_{\text{puri}}^{\text{BCNOT}} \sim 10.6$ ns and $\tau_{\text{puri}}^{\text{BISWAP}} \sim 5.5$ ns, for a qubit dephasing time of 500 ns. Depending on the measurement time, we can probably carry out more than one purification process well within the qubit coherent time. After the purification process, we measure the source qubits. If the measured results are in the $|\uparrow\uparrow\rangle$ or $|\downarrow\downarrow\rangle$ state, we can expect that the entangled state has been improved. Otherwise, we restart the whole process by again preparing mixed states for the two pairs.

(4) For charge qubits based on capacitively coupled single-electron QDs, the interqubit XY interaction appears in a rotating reference frame when an oscillating gate bias is applied [23]. For coupled QDs where the radius of each QD is about 2.5 nm and the distance between qubits is about 12 nm, $J \sim 0.1$ meV and $\omega_{\text{rot}} \sim 0.8$ meV. If we assume that we can switch on and off the coupling between QDs, we have $\tau_{\text{puri}}^{\text{BCNOT}} \sim 85.3$ ps and $\tau_{\text{puri}}^{\text{BISWAP}} \sim 48.7$ ps for a dephasing time of 100 ns [24].

VII. DISCUSSION

We have shown how to effectively reduce the number of operational steps in the purification protocol. In any stage of quantum communication, all efforts to speed up each process are strongly recommended from the viewpoint of finite coherence time as well as user satisfaction. The recent cavity-QED techniques using superconducting circuits have realized strong coupling between the cavity mode and the qubit

[6,7]. The present method of reducing the number of operations is effective for all qubits with XY interaction and would be of great use to realize quantum communication.

One possible quantum-communication system contains local quantum computers based on the cavity-QED mechanism and an optical fiber using photons. This is because the optical fibers would be the lowest-cost and most effective medium between distant parties, and the cavity-QED mechanism is effective for connecting photon to a local electronic system [25]. Thus, an effective transformation between local quantum states and photons is desirable. Houck *et al.* [7] have succeeded in controlling microwave photons in a superconducting circuit based on charge qubits. On the other hand, QDs are also good resources for entangled photon states [26]. More experiments regarding the emission and absorption of photons between the local cavity-QED system and the external photonic system are desired.

In Sec. VI, we have shown four examples of applications of the proposed purification protocols to solid-state qubits. The bottom line for using the purification protocol is whether we can prepare mixed states in which the probability of the desired Bell state is more than 1/2. At the first stage of quantum communication, we try to generate desired entangled states. However, those states are mostly imperfect and decohere gradually. If the probabilities of those entangled states are more than 1/2 even after passing through noisy channels, we can apply the purification protocol on those impure pairs. In order to repeat the next purification process, the time $\tau_{\text{puri}}^{\text{BISWAP}} + \tau_{\text{meas}}$ should be sufficiently smaller than the coherence time (τ_{meas} is the measurement time for judging the two-qubit states, which is, for example, 1–10 ms in Ref. [22]). Otherwise, it is possible that the revised fidelity obtained by the purification is smaller than that of the original state. In the third example in Sec. VI, for the second purification process, we have to generate a new mixed state from the measured qubits (called source qubits). The measured qubits are in a product state $|\uparrow\downarrow\rangle$ or $|\downarrow\uparrow\rangle$. First, we try to make a desired entangled state using the method mentioned in Sec. V. If the noisy environment successfully changes the imperfect entangled state into a mixed state with $A > 1/2$ in Eq. (29), we can proceed to the next purification. Otherwise, we have to apply random B^x , B^y , and B^z rotations. Because it takes a time τ_{rot} for each rotation, the total time to carry out the second purification process is given by $\tau_{\text{Bell}}^{\text{ISWAP}} + n_{\text{rot}}\tau_{\text{rot}}$ ($n_{\text{rot}} \geq 0$ is an integer for the randomization). This time should be smaller than that of the coherence time of the other surviving qubit (called the target qubit) that is waiting for the new entangled qubit. Whether these purification protocols succeed or not seems to strongly depend on the decoherence mechanism.

In this paper, we did not include any quantum error-correcting code in the purification protocol. This is because the quantum error-correcting code requires many qubits, in contrast to the current experimental situation with very few solid-state qubits. How to effectively combine the proposed purification process with the various quantum error-correcting codes would be an important issue for future studies.

VIII. SUMMARY

In summary, we have constructed an efficient adaptation of the entanglement purification protocols for qubits with XY interactions. Specifically, we show that the conventional CNOT gate, which requires turning on two-qubit interactions twice, can be replaced by a single i SWAP gate together with single-qubit rotations. This simplification of the gate pulse sequence reduces the time for entanglement purification and increases the robustness of the protocols. Our method could be used for any qubits with XY interactions, particularly cavity-coupled qubits, which allows solid-state qubits to be more easily integrable into a quantum-communication network.

ACKNOWLEDGMENTS

F.N. and X.H. are supported in part by the U.S. National Security Agency, Laboratory for Physical Sciences, Army Research Office, and the National Science Foundation. We thank A. Nishiyama, S. Fujita, and S. Ishizaka for useful discussions. K.M. acknowledges the support by the Incentive Research Grant at Riken.

APPENDIX: XY MODEL

Here, we summarize the derivation of the XY interaction between qubits in a cavity [5,6,15]. The Hamiltonian of two qubits in a cavity is given by the Jaynes-Cummings Hamiltonian:

$$H_{\text{JC}} = \omega a^\dagger a + \sum_{i=1}^2 \left\{ \frac{\omega_{qi}}{2} \sigma_i^- + (\chi_i \sigma_i^+ a + \text{H.c.}) \right\}, \quad (\text{A1})$$

where the qubit operators are defined by $\sigma_i^- = |e\rangle_i \langle e|_i - |g\rangle_i \langle g|_i$, $\sigma_i^+ = |e\rangle_i \langle g|_i$, and $\sigma_i^- = |g\rangle_i \langle e|_i$ using the ground $|g\rangle_i$ and first excited $|e\rangle_i$ states. In order to derive the two-qubit interaction, a unitary transformation $U = \exp(S)$ with

$$S = \sum_{i=1,2} \alpha_i (a^\dagger \sigma_i^- - a \sigma_i^+) \quad (\text{A2})$$

is introduced. For small parameters α_1 and α_2 , the Hamiltonian is transformed in second order in S such that

$$H'_{\text{JC}} = e^S H_{\text{JC}} e^{-S} \approx H_{\text{JC}} + [S, H_{\text{JC}}] + \frac{1}{2} [S, [S, H_{\text{JC}}]]. \quad (\text{A3})$$

The value of α_i ($i=1,2$) is determined such that the linear coupling terms between a and σ^\pm are deleted and $\alpha_i = \chi_i / \Delta_i$ with

$$\Delta_i = \omega - \omega_{qi}. \quad (\text{A4})$$

Then, we have

$$H'_{\text{JC}} \approx \omega a^\dagger a + \sum_{i=1}^2 \frac{\tilde{\omega}_q}{2} \sigma_i^- + \frac{\chi_1 \chi_2 (\Delta_1 + \Delta_2)}{2 \Delta_1 \Delta_2} (\sigma_1^+ \sigma_2^- + \sigma_1^- \sigma_2^+)$$

with

$$\tilde{\omega}_q = \omega_{qi} + \chi_i^2 / \Delta_i. \quad (\text{A5})$$

Thus we obtain the XY model from the Jaynes-Cummings model with interaction strength of

$$J = [\chi_1 \chi_2 (\Delta_1 + \Delta_2)] / (4 \Delta_1 \Delta_2). \quad (\text{A6})$$

-
- [1] C. H. Bennett, G. Brassard, C. Crepeau, R. Jozsa, A. Peres, and W. K. Wootters, Phys. Rev. Lett. **70**, 1895 (1993).
 [2] A. K. Ekert, Phys. Rev. Lett. **67**, 661 (1991).
 [3] C. H. Bennett, G. Brassard, S. Popescu, B. Schumacher, J. A. Smolin, and W. K. Wootters, Phys. Rev. Lett. **76**, 722 (1996); C. H. Bennett, D. P. DiVincenzo, J. A. Smolin, and W. K. Wootters, Phys. Rev. A **54**, 3824 (1996).
 [4] D. Deutsch, A. Ekert, R. Jozsa, C. Macchiavello, S. Popescu, and A. Sanpera, Phys. Rev. Lett. **77**, 2818 (1996).
 [5] A. Imamoglu, D. D. Awschalom, G. Burkard, D. P. DiVincenzo, D. Loss, M. Sherwin, and A. Small, Phys. Rev. Lett. **83**, 4204 (1999).
 [6] J. Q. You and F. Nori, Phys. Today **58**(11), 42 (2005).
 [7] A. A. Houck, D. I. Schuster, J. M. Gambetta, J. A. Schreier, B. R. Johnson, J. M. Chow, L. Frunzio, J. Majer, M. H. Devoret, S. M. Girvin, and R. J. Schoelkopf, Nature (London) **449**, 328 (2007).
 [8] J. Johansson, S. Saito, T. Meno, H. Nakano, M. Ueda, K. Semba, and H. Takayanagi, Phys. Rev. Lett. **96**, 127006 (2006).
 [9] J. Q. You and F. Nori, Phys. Rev. B **68**, 064509 (2003).
 [10] N. Schuch and J. Siewert, Phys. Rev. A **67**, 032301 (2003).
 [11] G. Burkard, D. Loss, D. P. DiVincenzo, and J. A. Smolin, Phys. Rev. B **60**, 11404 (1999).
 [12] W. Dür, H. J. Briegel, J. I. Cirac, and P. Zoller, Phys. Rev. A **59**, 169 (1999).
 [13] T. Tanamoto, Y. X. Liu, X. Hu, and F. Nori, e-print arXiv:0804.2290.
 [14] H. J. Briegel and R. Raussendorf, Phys. Rev. Lett. **86**, 910 (2001); R. Raussendorf and H. J. Briegel, *ibid.* **86**, 5188 (2001); R. Raussendorf, D. E. Browne, and H. J. Briegel, Phys. Rev. A **68**, 022312 (2003).
 [15] Y. X. Liu, C. P. Sun, and F. Nori, Phys. Rev. A **74**, 052321 (2006).
 [16] K. Maruyama and F. Nori, Phys. Rev. A **78**, 022312 (2008).
 [17] M. Grajcar, Y. X. Liu, F. Nori, and A. M. Zagorskin, Phys. Rev. B **74**, 172505 (2006).
 [18] A. O. Niskanen, K. Harrabi, F. Yoshihara, Y. Nakamura, and J. S. Tsai, Phys. Rev. B **74**, 220503(R) (2006).
 [19] S. Ashhab, S. Matsuo, N. Hatakenaka, and F. Nori, Phys. Rev. B **74**, 184504 (2006); S. Ashhab and F. Nori, *ibid.* **76**, 132513 (2007).
 [20] Y. X. Liu, L. F. Wei, J. S. Tsai, and F. Nori, Phys. Rev. Lett. **96**, 067003 (2006).
 [21] T. Yamamoto, M. Watanabe, J. Q. You, Y. A. Pashkin, O. Astafiev, Y. Nakamura, F. Nori, and J. S. Tsai, Phys. Rev. B **77**,

- 064505 (2008).
- [22] A. Izmalkov, M. Grajcar, E. Il'ichev, Th. Wagner, H.-G. Meyer, A. Yu. Smirnov, M. H. S. Amin, Alec Maassen van den Brink, and A. M. Zagorskin, *Phys. Rev. Lett.* **93**, 037003 (2004).
- [23] T. Tanamoto, *Phys. Rev. A* **64**, 062306 (2001).
- [24] W. G. van der Wiel, S. D. Franceschi, J. M. Elzerman, T. Fujisawa, S. Tarucha, and L. P. Kouwenhoven, *Rev. Mod. Phys.* **75**, 1 (2002).
- [25] J. I. Cirac, P. Zoller, H. J. Kimble, and H. Mabuchi, *Phys. Rev. Lett.* **78**, 3221 (1997).
- [26] R. M. Stevenson, R. J. Young, P. Atkinson, K. Cooper, D. A. Ritchie, and A. J. Shields, *Nature (London)* **439**, 179 (2006).